QUANTUM MECHANICAL STUDY OF DIFFERENT TYPES OF NUCLEIC ACID SENSORS

SUMMARY OF THE THESIS

THESIS SUBMITTED FOR THE AWARD OF THE DEGREE OF

Doctor of Philosophy

in

Applied Physics

By

Asheesh Kumar

Enrolment No.: 594/11

Under the Supervision of

Prof. Devesh Kumar

Department of Applied Physics

School for Physical Sciences

Babasaheb Bhimrao Ambedkar University, Lucknow,

U.P., (India) – 226025

March, 2019

Quantum Mechanical Study of Different Types of Nucleic Acid Sensors

SUMMARY

Chapter 1: Introduction

Nucleic Acid

Nucleic acids are biomolecules which are essential for all known forms of life. Nucleic acids were named for their initial discovery within the nucleus, and for the presence of phosphate groups (related to phosphoric acid). Nucleic acids (DNA and RNA) perform a variety of crucial functions in organisms. DNA stores and transfers genetic information, it serves as a template for the synthesis of new DNA and RNAs, while RNAs carry out protein synthesis. Nucleic acids contain only a few different components, but they have great structural diversity.

Structures of Nucleic Acids

There are two classes of nucleic acids, viz, DNA (Deoxyribonucleic acid) and RNA (Ribonucleic acid).

Pyrimidines in DNA and RNA: (Cytosine and Uracil in RNA, Cytosine and Thymine in DNA)

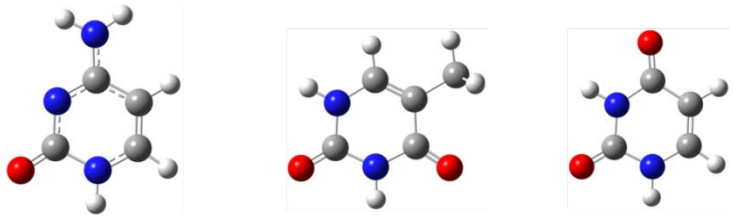

Figure 1: Optimized Structures of pyrimidine.

Purine is an aromatic organic compound that consists of a pyrimidine ring and an imadazole ring ($C_3H_4N_2$).

Purines in DNA and RNA: Adenine (A) and Guanine (G) are the purines.

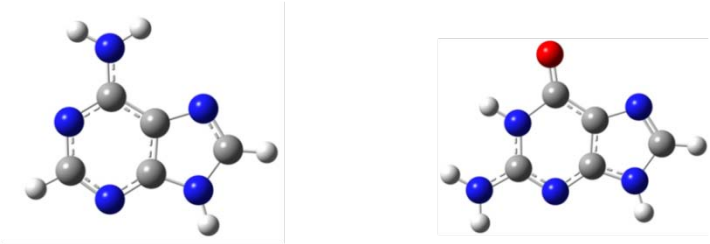

Figure 2: Optimized Structures of purines.

Allotropes of carbon

Although carbon had been known since many centuries but the main breakthrough in the field of carbon sciences is noteworthy after the discovery of fullerenes, carbon nanotubes (CNTs), and graphene.

The youngest allotrope of carbon, graphene, has a planar arrangement of carbon atoms that are packed in a two-dimensional hexagonal lattice fashion. Andre Geim and Konstantin Novoselov were jointly awarded with the nobel prize in 2010 for graphene. Its extended honeycomb network is the basic building unit of other important carbon allotropes such as 3D graphite that is formed by the stacking of several layers of graphene, 1D nanotube, formed by rolling the graphene and 0D fullerene that may be obtained by wrapping of graphene.

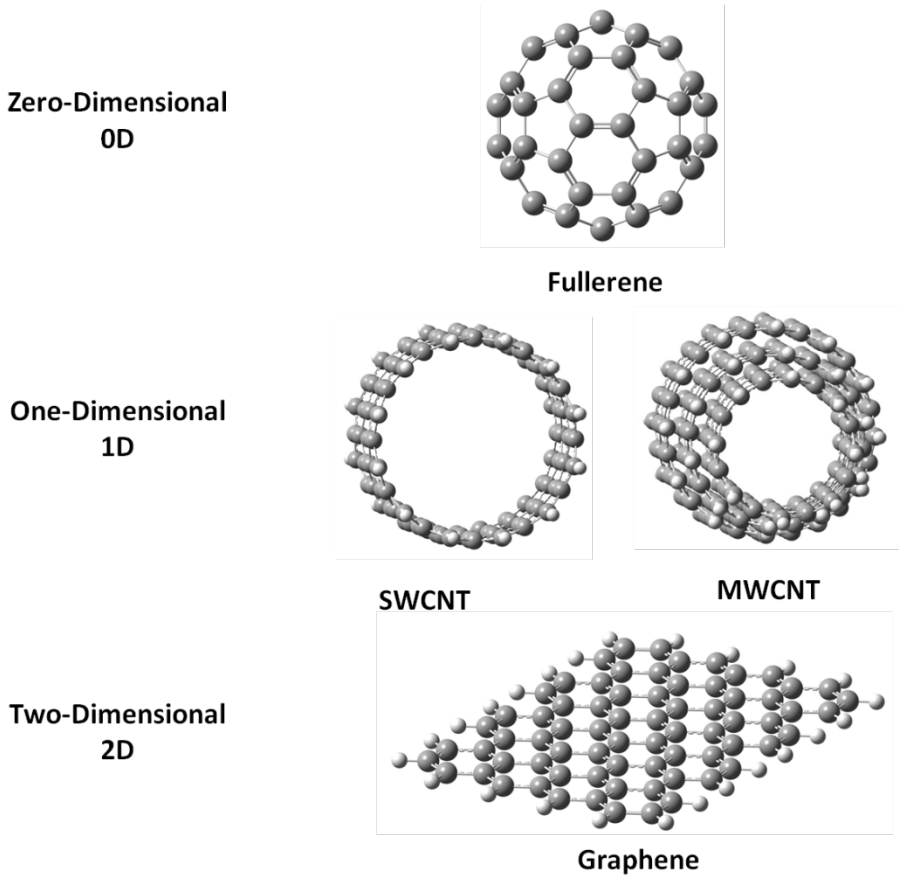

Figure 3: Structures of carbon allotropes.

Graphene

Graphene is a mono-atom-thick planar sheet of carbon atoms with sp^2 hybridization exquisitely organized in a honeycomb lattice. This is the thinnest material that can be imagined in the universe. Though it is the lightest known (density of 0.77 mg/m^2) material yet it is the strongest material measured, with strength nearly 100-300 times higher in comparison to steel. On account of its astounding structural and physicochemical properties, this exhilarating novel material quickly instigated mammoth interest in many disciplines like energy storage and conversion, field emission display, high-frequency electronics and nanoelectronics and transparent conductors.

Effect of Doping in graphene

Significant implementation of graphene is electronic devices that demands graphene to perform diverse electronic functions. Therefore, tuning the electronic properties of graphene is quite essential. Therefore doping by different procedures like hetero-atom substitution, edge functionalizations, chemical adsorption and defects were found to be efficacious in order to tune the electronic properties. With the doping of N- or B-atoms, the single walled carbon nanotube (SWCNT) may behave as n-type or p-type respectively. Doping can also transmute the electrical properties of graphene. Employing the ab-initio methodology, Martins et al., exemplified the presence of boron atom at the GNR edges which may be the cause of metal to semiconductor transition. Not only this, they also recommended that with suitable doping, the electronic current can also be fine tuned.

Biosensors

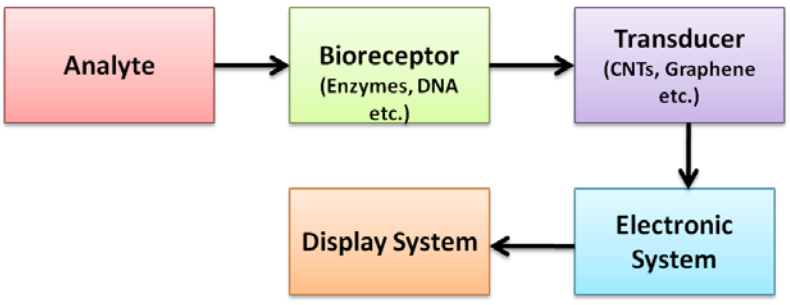

Figure 4: Block diagram of a biosensor.

Analyte: It is a substance of our interest that needs detection. For example, glucose is an 'analyte' in a biosensor to detect glucose level in a sample.

Bioreceptor: It is a molecule that particularly identfies the analyte and is termed as a bioreceptor. A bioreceptor may be an enzyme, aptamer, antibody, deoxyribonucleic acid (DNA) etc.

Transducer: The transducer is the main part of a biosensor and converts one form of energy into another. In a biosensor the role of the transducer is to convert the bio-recognition event into a measurable signal. As a transducer different carbon nanostructures can be used such as carbon nanotubes and graphene.

Electronics System: This is the part of a biosensor that processes the transduced signal and generates it for display. This system is comprised of complex electronic circuits that execute signal conditioning such as amplification and conversion of signals from analogue into the digital form.

Display System: The display consists of a user interpretation system such as the liquid crystal display of a computer or a direct printer that generates numbers or curves understandable by the user. The output signal on the display can be numeric, graphic, tabular or an image, depending on the requirements of the end user.

Detection of nucleic acid

For the detection of single stranded DNAs (ssDNA), and double stranded DNAs (dsDNA), its subunits like nucleobases, nucleotides, graphene has been used for sensitive and selective electrochemical detection. Such predictions with the aid of DNA sensors paved a new way for the DNA sequencing and DNA analysis. The four nucleobases (Adenine, Cytosine, Guanine, Thymine and Uracil) have distinct oxidation potentials. Huang et al. with the help of reduced graphene oxide and functionalizing it with –COOH groups electrochemically detected Guanine and Adenine. Hypoxanthine is a purine

derivative. A sensor to detect hypoxanthine was constructed using reduced graphene oxide (rGO).

Non-covalent interaction

The covalent bond is said to be formed between the two proximate atoms as a result of electron sharing between them. The idea of covalent bonding was traced many years earlier where different authors furnished a deeper intuition to the covalent bonds. One of the prospective implementation of non-covalent interaction in the field of biology is the field of drug delivery system. For their distinguished work in supramolecular chemistry, in 1987, Jean-Marie Lehn and Charles J. Pedersen, were jointly awarded the prestigious Nobel prize in chemistry, which mainly involves noncovalent type of interactions. Since then, this interaction has been studied extensively.

Stacking interaction

When the two aromatic entities are placed parallel or in perpendicular orientation then the interaction that exists between these two moieties are said to exhibit the stacking interaction (π- π) and CH- π type of interaction. Few examples that illustrate that the stacking interaction play a role of central importance are: (a) Vertical base-base interaction which stabilizes the double helical structure of DNA., (b) Conformational preference and binding of macrocyclic compounds like diarylnaphthalenes, (c) Complexation in host-guest systems, (d) Catalytic hydroformylation, (e) Catalytic formation of elastomeric polypropylene, (f) Asymmetric cis dihydroxylation of olefins, (g) Drug-receptor interactions etc.

Cation-π interactions

Cation-π interaction is a strong noncovalent interaction which exists between a cation and a π-system. Kebarle et al. made the first evaluation of K^+ ion interaction with benzene and have effectively manifested that K^+ ion shows a small preference to bind to benzene in comparison to the water molecule. The presence of cation-π interactions in biological systems and their relevance was demonstrated by many groups.

Chapter 2: Methodology

The interplay between theory and experiment can well be experienced with the help of the computational power. The computational modelling has emerged as a new paradigm beside theory and experiment. In the field of molecular sciences, computation has enabled us to provide basic insights at atomic level. The advances in recent computer software and hardware techniques enable to implement a range of computational methodologies in efficient and user friendly fashion. An attempt has been made to give a brief description of various theoretical methodologies employed. At the outset a brief introduction about the quantum mechanical principles, which provide platform to build the computational techniques, has been discussed.

Unlike molecular mechanics, quantum mechanics describes molecules in terms of interactions among nuclei and electrons. Quantum mechanics based methods are generally more accurate than MM methods, however, calculations are computationally more intensive than MM calculations. Three major categories of quantum mechanics are: ab initio, semi-empirical and density functional theory (DFT) methods.

We have used Gaussian program along with GaussView software package for all DFT calculations. Gaussian is the most popular commercial quantum chemistry package, currently distributed by Gaussian Inc. Wallingford, USA. The current version of the program is Gaussian 09. Gauss-View is popular modeling and visualization software of Gaussian. This program was developed by Semichem Inc., but distributed with Gaussian. Gauss-View is used to model the molecular system, create input and visualize the output. Gaussian processes the input created by Gauss View and is used to perform all calculations and produces an output. There are several other packages that can be used to visualize Gaussian outputs apart from Gauss View, some of them are Avogadro, Chemcraft etc.

AIM200 is a user friendly and efficient program, based on quantum theory of atoms in molecules. It uses the output generated by Gaussian 09 as an input.

Chapter 3: Binding of nucleic bases adsorbed on graphene (GR) and boron nitride graphene (BNG)

Graphene, the wonder material, since its discovery in 2004 by Andrew Geim and Novoselov has ignited the interest among the researchers due to its diverse chemical and physical properties that has led to a boom in the technological advancement.

In the present work, a detailed comparison between the pristine and the boron nitride graphene has been performed, the interaction of the nucleic bases with boron nitride has been studied in two modes that: (a) parallel mode and perpendicular mode with the boron nitride graphene. The HOMO-LUMO gap is also calculated.

The graphene sheet considered in the study, consist of 72 carbon atoms which were passivated with 24 hydrogen atoms at the boundaries. The boron nitride graphene is obtained with the help of the Gauss View 5.0 by substituting the Nitrogen and Boron atoms alternatively. Initially the graphene sheets i.e. the pristine graphene (GR) and the boron nitride graphene (BNG) were optimized by using the density functional theory (DFT) as implemented in the Gaussian 09 software package. The nucleic bases (NBs) were also optimized separately. The complex of the graphene and the nucleic bases were optimized at the same level using the B3LYP method and 6-31G basis set.

The present chapter can be well understood into three schemes: (scheme 1 which is comprised of the pristine graphene and the nucleic bases, scheme 2 consists of the boron nitride graphene and the nucleic bases that were made to interact in parallel configuration, while the scheme 3 deals with the boron nitride and the nucleic bases, in this scheme nucleic bases were made to interact in the perpendicular configuration).

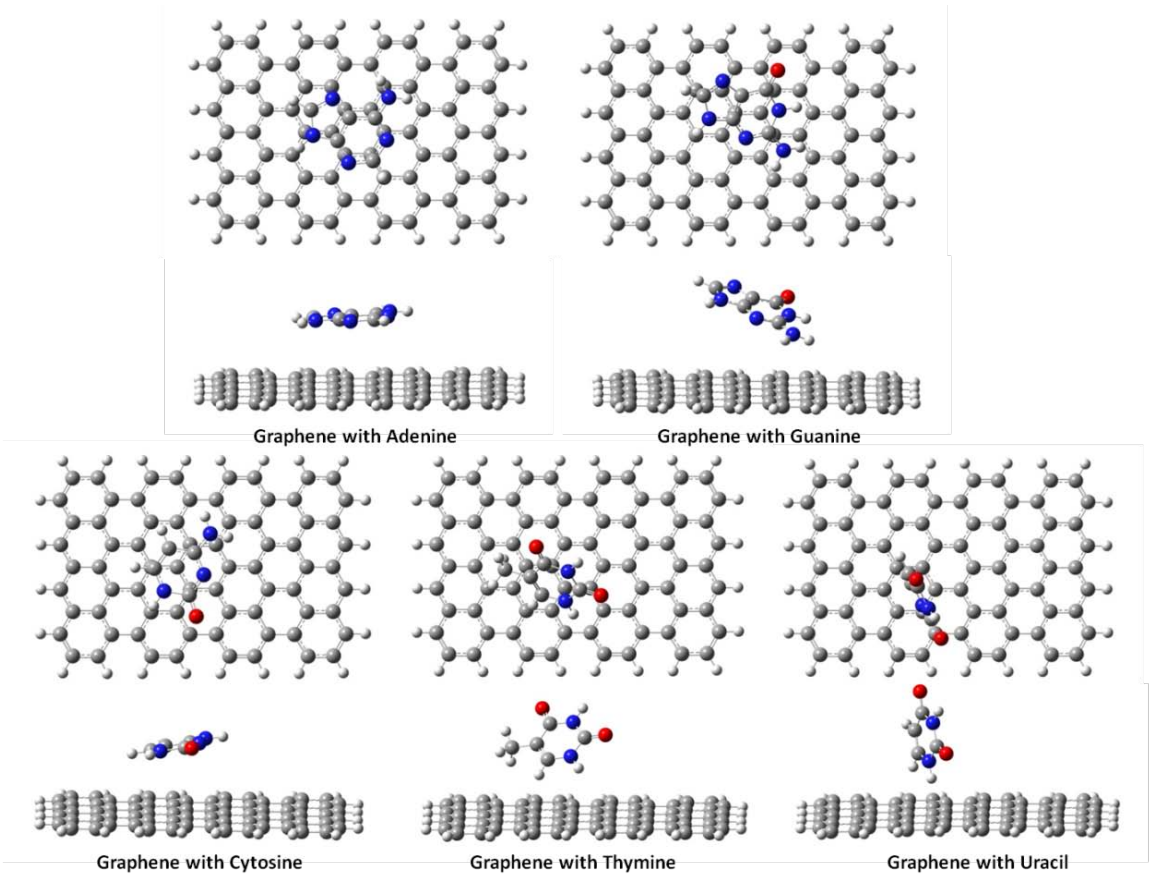

Figure 5: Pictorial representations of the nucleic bases interacting with pristine graphene in parallel position (top and side view).

Table 1: Calculated binding energy (in Kcal/mol) of pristine graphene (GR) and nucleic bases at (BS1, B3LYP/6-31++G** // B3LYP /6-31G) and (BS2, WB97XD/ 6-31++G** // B3LYP /6-31G).

Model System	**Nucleic bases(NBs)**	**Binding Energy (BS1, B3LYP/ 6-31++G**)**	**Binding Energy (BS2, WB97XD/6-31++G**)**
(Graphene)	Adenine (A)	-1.580	-12.700
	Cytosine (C)	-2.177	-12.695
	Guanine (G)	-2.858	-11.556
	Thymine (T)	-1.141	-9.450
	Uracil (U)	-3.449	-9.962

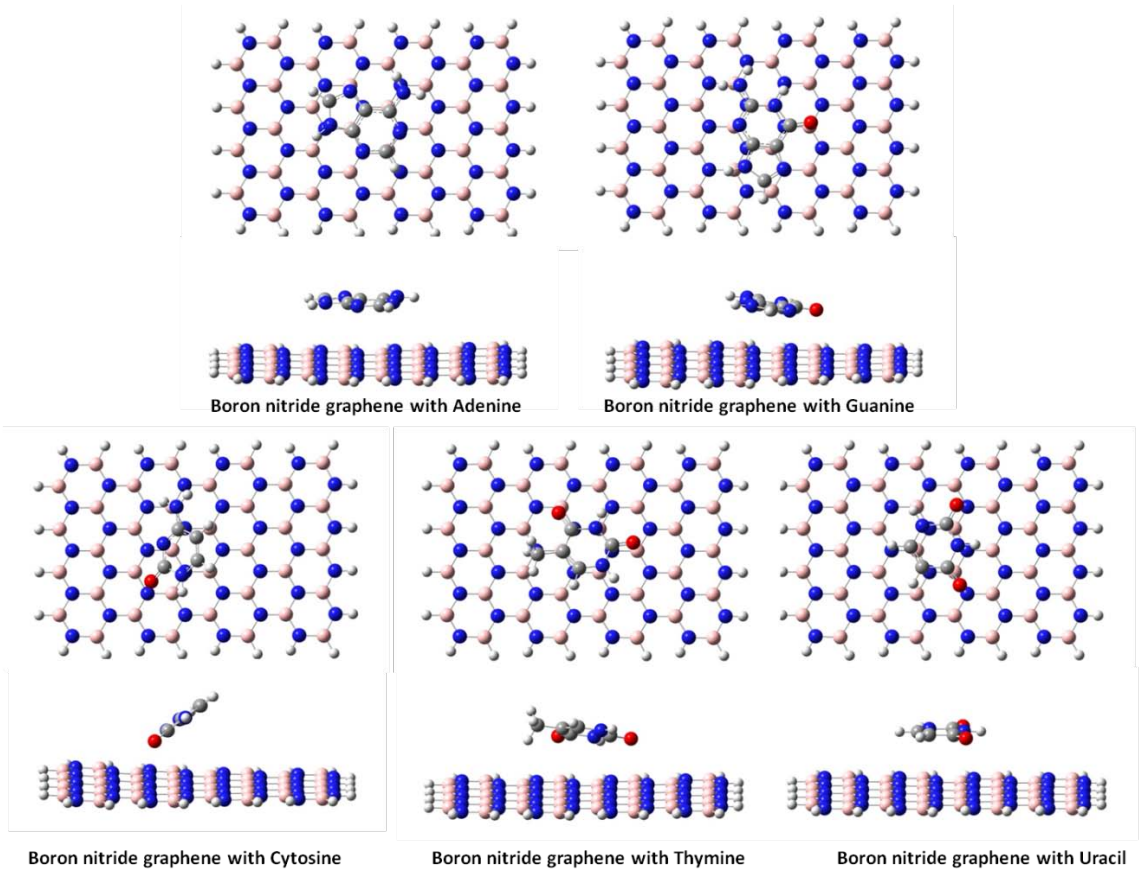

Figure 6: Pictorial representations of the nucleic bases interacting with boron nitride graphene (BNG) in parallel position (top and side view).

Table 2: Calculated binding energy (in Kcal/mol) of Boron Nitride Graphene (BNG) and nucleic bases in parallel mode of interaction at (BS1, B3LYP/6-31++ G** // B3LYP /6-31G) and (BS2, WB97XD/ 6-31++G** // B3LYP /6-31G).

Model System	**Nucleic bases(NBs)**	**Binding Energy (BS1, B3LYP/6-31++G**)**	**Binding Energy (BS2, WB97XD/6-31++G**)**
Boron Nitride Graphene	Adenine (A)	-.0123	-14.863
	Cytosine (C)	-2.430	-13.375
	Guanine (G)	-0.572	-17.689
	Thymine (T)	-0.552	-13.603
	Uracil (U)	-0.003	-12.183

In the present chapter, a systematic study has been accomplished to examine the binding energy values using highly reliable first principle calculations for the five known

nucleobases with the graphene and boron nitride graphene. The analysis reveals that NBs seems to have a substantially high preference for binding in the π−π stacking fashion. The preferential order of binding of the nucleic bases performed in scheme 1 of this chapter with basis set B3LYP/631++G is in agreement with the experimental study performed by Albertorio et al. It is also quite noteworthy that the calculations performed in the scheme 2 with basis set WB97XD/631++G are in agreement with other computational studies performed earlier. The electronic properties of these molecules are also evaluated with the help of reactive surfaces such as HOMO, LUMO and MESP. The observations obtained in this chapter should encourage a more focused research on graphene for the possible applications for nucleic acid sensors and DNA sequencing.

Chapter 4 : Interaction of modified nucleic bases (MNBs) with graphene and doped graphenes

Graphene, a versatile material has opened new avenues to increase the technological advancement owing to its extraordinary properties and enormous application in various fields. Therefore, the application of graphene and its derivatives in various fields like sensors, field effect transistors, nanoelectronics, engineering nanocomposite materials, energy storage, biology, catalysis, and medicine have been studied extensively. Umadevi et al. used the density functional theory and validated that the binding energy of carbon nanotube and DNA/RNA nucleic bases complexes is inversely proportional to the curvature. The DNA sequencing was observed successfully with the aid of functionalized graphene in order to distinguish the various nucleic bases. For the removal of pollutants and pesticides, graphene can be used effectively.

The model of the graphene consists of 42 carbon atoms that are passivated at the edges of the carbon atoms with hydrogen atoms. Thus, the molecular formula of graphene is $C_{24}H_{16}$. The density functional theory (DFT) methods like M06-2X and WB97XD were extensively used methods to study the non-covalent interactions. Therefore these functional are used for the present study. The geometry of the graphene is optimized at M06-2X/6-31+G** level of theory.

In the present study, the pristine graphene is doped with Aluminium, Sulfur, Nickel, Gallium, and Germanium atoms. The exact position of doping site is taken into consideration from the previous study. The doped graphene models were also optimized at the same level of theory. The modified nucleic bases (MNBs) i.e. caffeine, hypoxanthine, uric acid, and xanthine are abbreviated as CAF, HX, UA and X respectively in the following part of this chapter. The graphene models are abbreviated as pristine graphene (GR), Aluminium doped graphene (AlG), Sulfur doped graphene (SG), Nickel doped graphene (NiG), Gallium doped graphene (GaG), and Germanium doped graphene as (GeG).

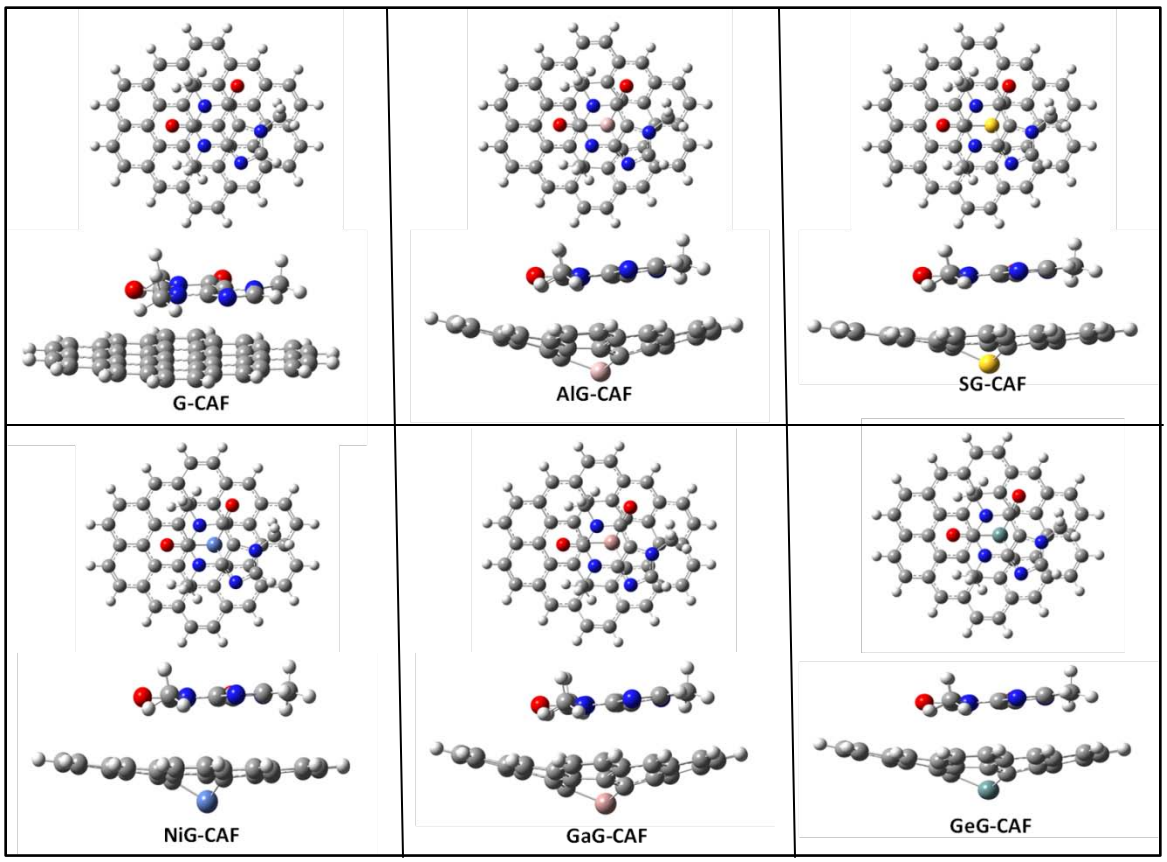

Figure 7: Optimized geometries of the complexes formed by caffeine with graphene and doped graphenes at M06-2X/6-31+G** level: top view and side view.

Table 3: Calculated interaction energy (kcal/mol) of MNBs with graphene models (GR, AlG, SG, NiG, GaG, GeG) at M06-2X/6-311++G** and WB97XD/6- 31++G** with and without basis set superposition error (BSSE).

Model	MNBs	BSSE Uncorrected M06-2X	BSSE corrected M06-2X	BSSE corrected WB97XD	BSSE corrected B3LYPD
GR	CAF	-26.280	-20.11	-23.63	-21.50
	HX	-19.456	-14.32	-16.93	-15.43
	UA	-23.087	-17.38	-19.31	-18.27
	X	-20.266	-14.98	-16.99	-15.76
AlG	CAF	-52.104	-46.58	-50.71	-50.57
	HX	-52.437	-47.33	-49.86	-50.13
	UA	-54.401	-49.15	-50.70	-51.40
	X	-53.176	-48.21	-50.17	-50.62
SG	CAF	-85.799	-79.68	-82.78	-80.98

	HX	-82.050	-76.77	-78.98	-77.65
	UA	-85.138	-79.52	-81.06	-79.70
	X	-81.562	-76.26	-77.99	-76.82
NiG	CAF	-96.185	-90.40	-92.04	-86.11
	HX	-91.613	-86.54	-87.77	-82.04
	UA	-95.735	-90.35	-90.51	-85.25
	X	-91.309	-86.28	-86.39	-81.19
GaG	CAF	-55.307	-50.27	-50.07	-51.90
	HX	-55.980	-51.35	-49.21	-51.50
	UA	-56.644	-51.24	-49.29	-51.79
	X	-54.780	-49.59	-47.61	-49.91
GeG	CAF	-48.750	-43.04	-47.68	-43.04
	HX	-48.00	-42.90	-46.01	-48.15
	UA	-49.284	-43.83	-46.26	-48.44
	X	-45.721	-40.59	-43.54	-45.77

AIM Analysis

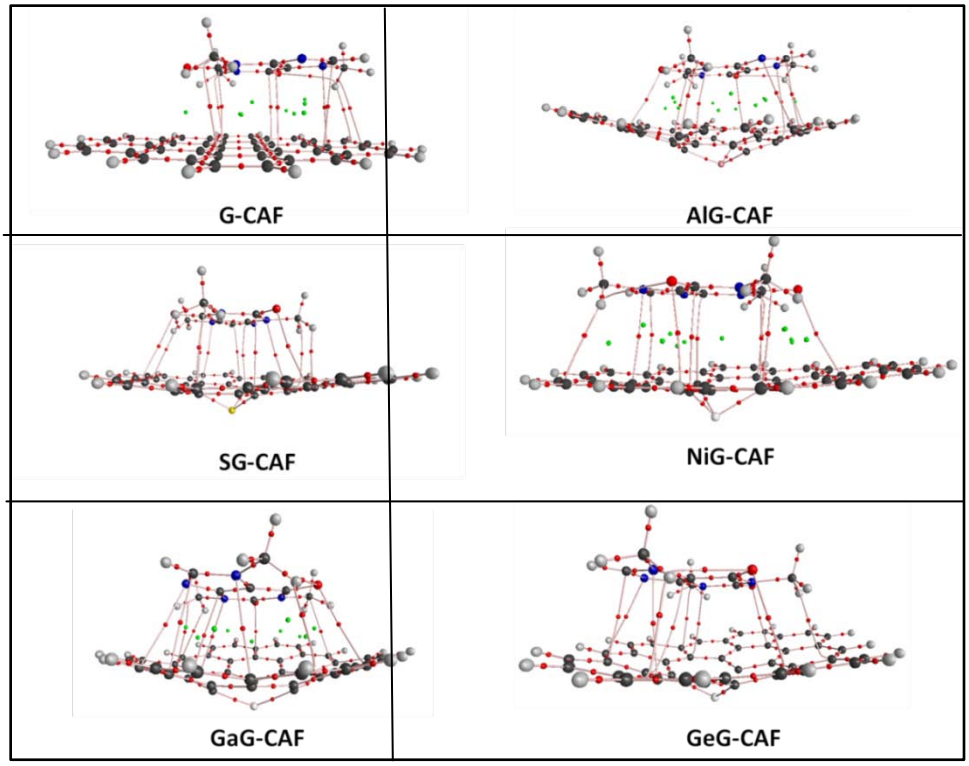

Figure 8 Molecular graphs of different complexes of graphene models with caffeine. The bond critical points (BCPs) are represented by red dots.

The molecular electrostatic potentials for the MNBs are shown in Figure 1. The active centers of these MNBs like CO and N were made to interact with the pristine graphene (GR) and doped graphene (AlG, SG, GaG and GeG). The active centers of the MNBs were placed parallel to the graphene surface at a certain distance around 3Å. The set of geometries obtained in this way were optimized at M06-2X/6-31+G** level. It is quite noteworthy that all the MNBs interacted with the different graphene models via the π-π (stacking) interaction. In almost all the complexes formed the doped atom protrudes out of the graphene surface. The interaction energies calculated at M06-2X/6-311+G** are shown in Table 1. The interaction energies were corrected for the basis set superposition error (BSSE). It is clear from the table that the BSSE uncorrected values are higher than the corrected values. Thus, clearly indicating the importance of the BSSE for the studied complexes. The BSSE corrected values for the BS1, BS2 and BS3 are also tabulated in the same table. Taking into consideration, the stacking pattern of the geometries, the dominant role of the dispersion interaction can be well understood.

Table 4: Calculated sums of electron density ρ and Laplacian $\nabla^2\rho(r_c)$ at the BCPs.

Model	**MNBs**	**Charge Density (ρ)**	**Laplacian of (ρ)**
G	CAF	0.07	-0.06
	HX	0.05	-0.04
	UA	0.06	-0.05
	X	0.05	-0.04
AlG	CAF	0.07	-0.05
	HX	0.07	-0.05
	UA	0.08	-0.06

	X	0.06	-0.05
SG	CAF	0.08	-0.07
	HX	0.06	-0.04
	UA	0.08	-0.06
	X	0.06	-0.05
NiG	CAF	0.07	-0.06
	HX	0.06	-0.05
	UA	0.07	-0.06
	X	0.05	-0.04
GaG	CAF	0.08	-0.06
	HX	0.07	-0.05
	UA	0.07	-0.05
	X	0.07	-0.05
GeG	CAF	0.07	-0.06
	HX	0.05	-0.04
	UA	0.06	-0.05
	X	0.06	-0.04

The present study elaborates in detail the adsorption mechanism of modified nucleic bases (MNBs) on pristine graphene (GR) and various other models of doped graphenes (AlG, SG, NiG, GaG, GeG) considered in this study. The preferential order of interaction energy for the studied modified nucleic bases (MNBs) in general is CAF>UA>HX>X. The AIM analysis confirms that the MNBs interact with the π–π (stacking) interaction which is the main factor for the adsorption of MNBs on different doped graphenes. Significant changes in the HOMO-LUMO gap of the intermolecular complex are analyzed. These variations in the electronic structure and associated changes in the electronic properties will be helpful to design new sensors. Therefore, the findings of this study may spark experimental studies in this direction. This detailed study using electronic calculations and associated analysis tools have been used to explore the utilility of this study in the field of sensors.

Chapter 5: Interaction of alkali metal ions with zig-zag single walled carbon nanotube (SWCNT)

In the field of nanotechnology, the carbon nanotubes have contributed significantly at a large scale. For the last two decades or so, there has been a great deal of research for these carbon nanotubes in almost all possible areas but there are few yet to be explored. The word “nano” has been taken from the Greek which means “dwarf” (small) in English. During the last three decades, by utilizing the various scientific instruments, this branch of science “nanotechnology” has well established itself and has become a word of mouth among the entire research fields. The credit belongs to Norio Taniguchi, of Japan, who first named this famous branch of science, i.e. “Nanotechnology”. It is well known today that the credit goes to Sumio Iijima for the discovery of carbon nanotube in 1991 but there is a very interesting story (incident) about it.

The CNT have some prominent properties like high mechanical strength, high surface areas, and large aspect ratios. Yu et al. reported that the tensile strength of steel is 20 times lower than SWCNTs; also the Young’s modulus of CNTs is much greater than fibers of steel. Also the thermal and electrical conductivity of CNT is reported to be comparable with that of copper. These outstanding properties opened new avenues for the application of the carbon nanotubes in different fields. Guanghua et al. reported that the mechanical strength of SWCNTs depend on the diameter.

In the present era of advanced computational techniques, the relevance of the non-covalent interactions can be well understood as they have brought themselves in lime light due to their commanding force in biological systems and various other important

fields. Non-covalent interactions were conventionally thought to be as weak interactions but have proven their presence in different fields. The hydrogen bonding is the most extensively examined interaction, yet the noteworthiness of the other noncovalent interactions like CH···π interactions, anion–π , cation–π, π–π stacking, and halogen bonding for a wide range of applications in material design, molecular recognition, catalysis, supramolecular interactions are well noticed.

The structure of the SWCNT in the present study has been considered from the previous study. There are 80 carbon atoms and 20 Hydrogen atoms present in the model system. The dangling bonds at the truncated ends of the SWCNT were passivated with hydrogen atoms to stop spurious end effects. The calculations performed in this chapter were carried out by using density functional theory (DFT) method as implemented in the Gassian09 program package. In this study, the geometries of alkali metal ions (K+, and Na+) with single walled carbon nanotube (SWCNT) were optimized using the well known B3LYP method at 6-31G* basis set. The single point energy calculations were also performed by using B3LYP which is abbreviated as (BS1) and M06 abbreviated as (BS2) method at 6-31++G** basis set.

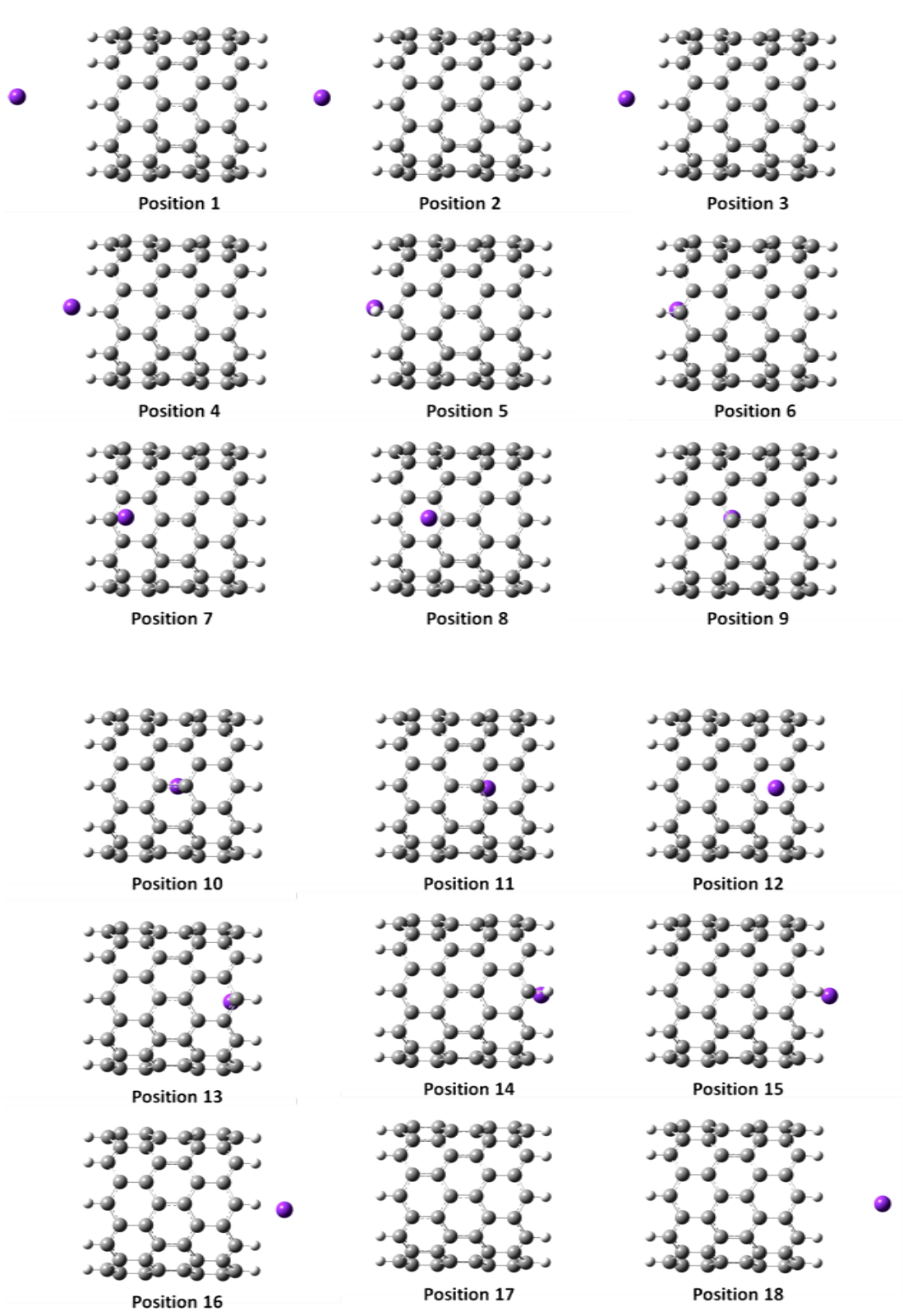

Figure 9: Optimized geometries of the complexes formed between the SWCNT(10,0) and alkali metal ion (K^+) at B3LYP/6-31G* method.

Table 5: Calculated Total Energy (Kcal/mol), Δ**E** (Kcal/mol), Homo Lumo Gap (eV) and Mulliken charge on alkali metal ion (K^+) and Single Walled Carbon Nanotube (SWCNT) at B3LYP/6-31++G** (BS1).

Metal ion	**Various Positions**	**Total Energy (Kcal/mol) BS1**	**$\Delta E=E_0-E$ (kcal/mol)**	**Homo Lumo Gap (eV)**	**Charge on K^+**	**Charge on CNT**
K^+	Position-01	-2296876.185	0.000	0.121	1.015	-0.015
	Position-02	-2296877.903	1.718	0.421	1.035	-0.035
	Position-03	-2296881.36	5.175	0.427	1.035	-0.035
	Position-04	-2296887.025	10.839	0.425	1.015	-0.015
	Position-05	-2296894.603	18.418	0.425	1.005	-0.005
	Position-06	-2296900.15	23.965	0.423	0.849	0.151
	Position-07	-2296901.588	25.403	0.418	0.835	0.165
	Position-08	-2296900.761	24.575	0.415	0.966	0.034
	Position-09	-2296900.026	23.840	0.414	0.996	0.004
	Position-10	-2296899.849	23.664	0.414	0.993	0.007
	Position-11	-2296900.354	24.169	0.415	0.993	0.007
	Position-12	-2296901.254	25.068	0.417	0.904	0.096
	Position-13	-2296901.16	24.975	0.422	0.800	0.200
	Position-14	-2296897.481	21.296	0.425	0.958	0.042
	Position-15	-2296890.312	14.127	0.426	1.017	-0.017
	Position-16	-2296883.419	7.234	0.425	1.025	-0.025
	Position-17	-2296879.141	2.956	0.424	1.045	-0.045
	Position-18	-2296876.707	0.522	0.244	1.023	-0.023

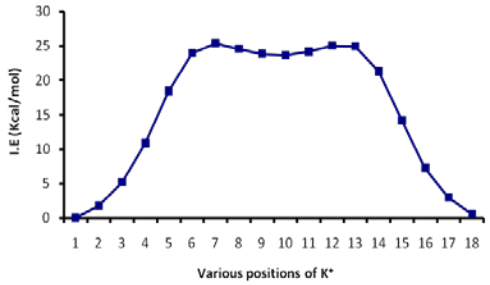

Figure 5.3Variation of the Interaction energy (kcal/mol) of complex system at different positions using B3LYP/6-31++G** (BS1)

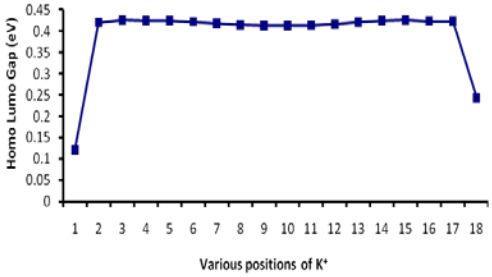

Figure 5.4 Variation of the Homo Lumo gap (eV) of alkali metal ion at different positions using B3LYP/6-31++G** (BS1)

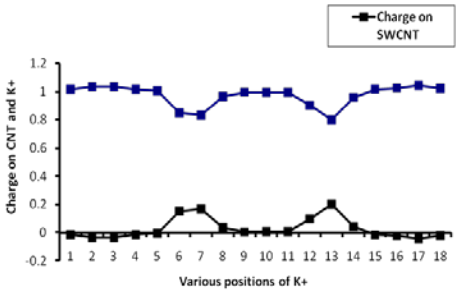

Figure 5.5 Mulliken charge analysis of SWCNT (10,0) and metal ion at different positions using B3LYP/6-31++G** (BS1)

Figure 10: Various graphs showing the variation of interaction energy, homo lumo gap, and mulliken charge analysis.

Table 6: Calculated Total Energy (Kcal/mol), ΔE (Kcal/mol), Homo Lumo Gap (eV) and Mulliken charge on alkali metal ion (K^+) and Single Walled Carbon Nanotube (SWCNT) at M06/6-31++G** (BS2).

Metal ion	Various Positions	Total Energy (Kcal/mol) BS2	$\Delta E=E_0-E$ (kcal/mol)	Homo Lumo Gap (eV)	Charge on K^+	Charge on CNT
K^+	Position-01	-2295443.757	0.000	0.504	0.937	0.063
	Position-02	-2295445.353	1.597	0.535	0.966	0.034
	Position-03	-2295448.845	5.088	0.553	1.012	-0.012
	Position-04	-2295455.72	11.963	0.553	1.041	-0.041
	Position-05	-2295464.877	21.120	0.554	1.044	-0.044
	Position-06	-2295471.319	27.562	0.548	0.904	0.096

	Position-07	-2295474.138	30.381	0.538	0.829	0.171
	Position-08	-2295473.127	29.371	0.531	0.903	0.097
	Position-09	-2295472.435	28.679	0.529	0.909	0.091
	Position-10	-2295472.209	28.453	0.528	0.943	0.057
	Position-11	-2295472.923	29.166	0.530	0.897	0.103
	Position-12	-2295473.86	30.103	0.534	0.880	0.120
	Position-13	-2295473.181	29.424	0.544	0.836	0.164
	Position-14	-2295468.155	24.398	0.552	1.013	-0.013
	Position-15	-2295459.512	15.755	0.555	1.049	-0.049
	Position-16	-2295451.343	7.586	0.549	1.026	-0.026
	Position-17	-2295446.617	2.860	0.542	0.984	0.016
	Position-18	-2295444.309	0.552	0.519	0.948	0.052

The present chapter is focussed upon the interaction of the alkali metal ion precisely the K^+ and Na^+ ions which were made to interact with the single walled SWCNT. There were a total of 18 different positions at which the metal ions were allowed to pass from one end of the SWCNT to the other. Certain important parameters like interaction energy, homo lumo energy gap, Mulliken charge analysis were observed as the metal ion enters and comes out from the other side of the SWCNT. Significant changes occur in the homo lumo gap which may help to tune the electronic and conducting properties of the SWCNT.

General conclusion and future prospects

The work done in the present thesis illustrates some striking focal points:

A. Technological advancements and recent developments in theory have enabled evolution of highly accurate, efficient and inexpensive methods applicable for designing novel sensors.

B. The extensively tested and highly benchmarked methods used by our research group were proven to be in congruence with experimental as well as theoretical studies accomplished in the past which proved be useful to study the interaction of graphene systems with nucleic bases presented in this thesis.

C. The studies present in this thesis work are expected to bridge the computational and experimental work being carried out with graphene and boron nitride graphene. Also they are expected to meet challenges of targeted drug delivery.

D. The focus of the study is to confirm the importance of DNA sequencing and specificity at molecular level. Thus, our study attempts to provide useful insights on the binding of nucleic base molecules to various carbon nanostructures.

E. Doping is an efficient way to tune the electronic properties of the graphene model system and its importance is highlighted in the present thesis.

Thus, the molecular modeling studies performed in the present thesis can be fruitful to design novel sensors, to understand DNA sequencing and to aid targeted drug delivery.